Dynamic and stress relaxation properties of the whole porcine temporomandibular joint disc under compression

Eva Barrientos[1], Fernández Pelayo [1*], Eiji Tanaka[2], María Jesús Lamela-Rey[1], Alfonso Fernández-Canteli [1]

[1] Department of Construction and Manufacturing Engineering, University of Oviedo, Spain.

[2] Department of Orthodontics and Dentofacial Orthopedics, Institute of Biomedical Sciences, Tokushima University Graduate School, Tokushima, Japan.

Running title: Compressive properties of the whole TMJ disc

Corresponding Author:

Pelayo Fernández

Assistant Professor

University of Oviedo

Departamento de Construcción e Ingeniería de Fabricación

Edo. Dep. Oeste. N-7. 7.1.23. CP: 33204 Gijón. España. (Spain)

E-mail: fernandezpelayo@uniovi.es

Abstract

In this study, the dynamic and static compressive properties of the whole porcine temporomandibular joint (TMJ) disc were investigated. The aim of the study was to develop a new simple method for the evaluation of joint viscoelasticity, enabling examination of the load-bearing capacity and joint flexibility of the entire disc. For the experiments, a novel testing fixture that reproduces the condylar and fossa surfaces of the TMJ was developed to replicate TMJ disc geometry. Ten porcine discs were used in the experiments. Each disc was dissected from the TMJ and sinusoidal compressive strain was applied to obtain the storage and loss moduli. Static strain control tests were carried out to obtain the relaxation modulus. The result of static and dynamic tests indicated that the whole disc presented viscoelastic behavior under compression. Storage and loss moduli increased with frequency and the relaxation modulus decreased over time. The loss tangent showed less frequency dependence, with values ranging from 0.2 to 0.3, suggesting that the viscous properties of the disc cannot be neglected. These results provide a better understanding of whole disc mechanical compression behavior under realistic TMJ working conditions.

Keywords: TMJ ; Temporomandibular Joint ; soft tissues ; viscoelasticity ; biomechanical characterization; experimental techniques.

1. Introduction

The temporomandibular Joint (TMJ), a diarthrodial synovial joint, is one of the most complicated joints in the human body. It consists of the mandibular condyle and the articular eminence and glenoid fossa of the temporal bone (Ingawalé and Goswami, 2009). Like other synovial joints, the TMJ enables large relative movements. Most dysfunctions, which affect around 15%-20% of the population, are related to the joint disc (Tanaka et al., 2008). The TMJ disc is fibrocartilaginous, with variable amounts of cells and extracellular matrix composed of macromolecules and fluid (Tanaka et al., 2008).

The mechanical properties of the TMJ disc have been studied extensively to improve understanding of the disc's mechanical behavior and of load transmission through it (Detamore and Athanasiou, 2003; Tanaka and van Eijden, 2003, Tanaka et al., 2014). During function, the TMJ disc is subjected to dynamic and static loads. The biomechanical properties of this disc are known to be region dependent (Pelayo et al., 2012).

When different regions (central, medial, lateral, anterior, and posterior) of disc sample are tested, unconfined and/or confined tests should be carried out (Kuo et al., 2010; Pelayo et al., 2012). Although both types of result can be used for comparison of parameters such as stiffness ratios or viscoelasticity among regions, little information is available about testing under more-realistic working conditions of the whole disc, e.g., the natural institutional flow of liquid between the regions and the behavior of complete (uncut) disc components. Moreover, the natural scatter of data due to differences among individuals may be influenced by factors introduced by the testing of cut disc specimens (e.g., lack of natural flow of liquid within regions, potential damage during specimen preparation, lack of parallels between specimen surfaces when testing with parallel plates) (Commisso et al., 2014).

All of these conditions often make it difficult to fit a reasonable mechanical material model of the disc that can be used for further calculations on the TMJ, such as numerical models constructed with the finite element (FE) method. The lack of experimental simulation data for the whole TMJ renders the validation of FE model results difficult (Chen et al., 1998; Tanaka et al., 2004; Pérez del Palomar and Doblaré, 2006). In this study, dynamic and static compressive properties of the whole porcine TMJ disc were investigated. The objective was to develop a new simple method for the evaluation of viscoelasticity in the whole TMJ disc, to enable the examination of load-bearing capacity and joint flexibility.

2. Materials and methods

2.1 Specimen preparation

Ten complete left TMJs from ten porcine heads (age 6-7 months, gender not specified) were obtained from a local slaughterhouse (Noreña, Asturias, Spain). One complete porcine head (age 6-7 months, gender not specified) was also obtained to test the fixture design procedure (see section 2.2). The Animal Care and Use Committee of the University of Oviedo, Spain, approved the experimental protocol.

The discs were dissected carefully after sacrifice and immersed in a physiologic saline solution (0.09 g NaCl/100 ml) in hermetic containers. They were frozen at -25°C until the experiments were conducted. The complete porcine head was allowed to cool after sacrifice and was transported in a portable refrigerator directly to the tomographic scanner.

2.2 Tooling design

To develop the tool needed to test the complete disc specimens, the complete pig head was scanned using three-dimensional (3D) Accuitomo 170 device (Morita Co., Kyoto, Japan). To create the 3D model, DICOM data files were processed using MIMICS software (Materialise, Leuven, Belgium), producing stereolithographic files. The surfaces were treated using Rhinoceros software (McNeel & Associates, Seattle, WA, USA). The tooling details needed to adapt the bones to the testing machine were designed in Solidworks (Dassault Systèmes, Paris, France). The 3D data was then used to program a numerical-control milling machine that accurately reproduced the fossa and condylar surfaces of a left TMJ. Aluminum alloy was used for the manufacture of the testing tool. The design of the testing tool and a schematic flow diagram of the tooling design procedure are presented in Figure 1.

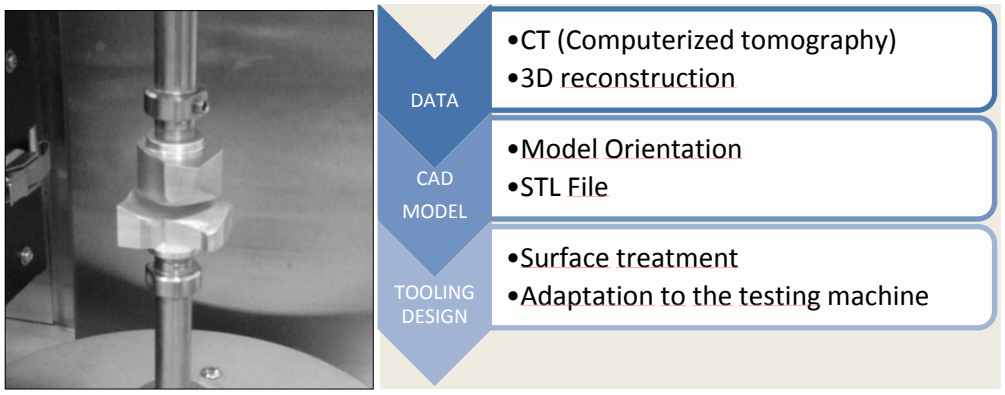

Figure 1. Design of the fixture tool used whole disc tests and steps in the manufacturing process. STL, stereolithographic.

2.3 Determination of effective cross-sectional area

Compression tests were conducted with the whole discs. The condyle fixture served as an indenter (Figure 1). Given the complex geometry of this indenter, the effective cross-sectional area (A_{eff}) for stress estimation ($\sigma = force/A_{eff}$) during testing could not be known *a priori*; an inverse characterization process using FE method was required to obtain A_{eff} (see section 2.3.2). For nonstandard cylindrical flat indenters (Zheng et al., 1999; Liu et al., 2004; Choi and Zheng, 2005), the effective cross-sectional area is known to depend on several factors, such as indenter diameter and indentation depth. This dependence can also differ among contact areas (A_cs). One can thus propose the existence of a scale factor, κ, which relates the contact area and the effective area ($A_{eff} = A_c/\kappa$) depending on the material properties. This factor must be determined to obtain the modulus of the material.

To obtain κ, an inverse material characterization technique using an FE model was adopted. To assess the reliability of the results, two parameters were used: an estimation of the experimental contact area between the condyle fixture and the disc and the measured force during whole-disc testing.

As the effective area (A_{eff}) was unknown, an arbitrarily selected area was used for initial testing. Then, the effective area of each disc was calculated, and introduced into the testing machine software (Orchestrator; TA Instruments, New Castle, DE, USA). The experimental results were updated based on the new area. Finally, the modulus of the material was obtained.

2.3.1 Experimental contact area estimation

To obtain the experimental contact area (A_c), each disc was sprayed with liquid petroleum jelly immediately after testing and 50% of the maximum load measured during testing was applied. The condyle tool was then removed from the machine and sprayed with a very fine white talc powder. The powder revealed the print of the contact area, which was photographed (Figure 2). The contact area was measured by overlapping the contact print and the 3D model of the condyle. Rhinoceros software was used to create a 3D polyline and a polysurface. This polysurface was compared with the photograph to ensure accuracy, and then measured to obtain the experimental cross-sectional contact area. The estimated average contact area for the 10 discs was 268.8 ± 9.4 mm^2.

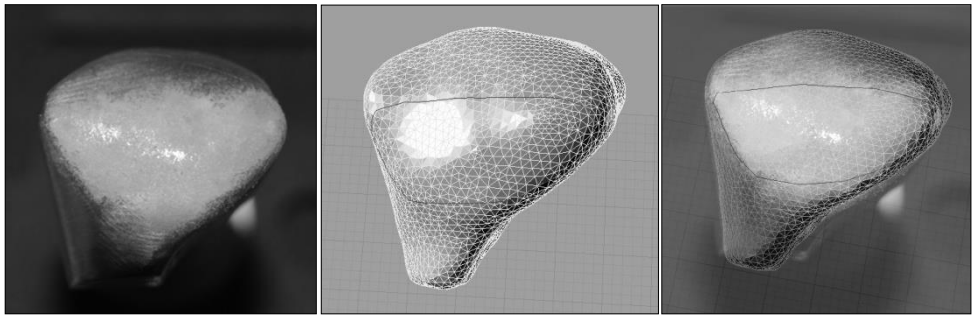

Figure 2. Procedure for obtaining the contact area (A_c) between the condyle (indenter) and the discs. From the left to the right: Condyle tool with the print of the contact area; 3D model of the condyle with the 3D polyline used; Overlap of the Real print and the 3D print.

2.3.2 Inverse material characterization using a finite element model

For inverse characterization, an FE model simulating the experiments was assembled using ABAQUS software (Dassault Systèmes, Paris, France) (Figure 3).

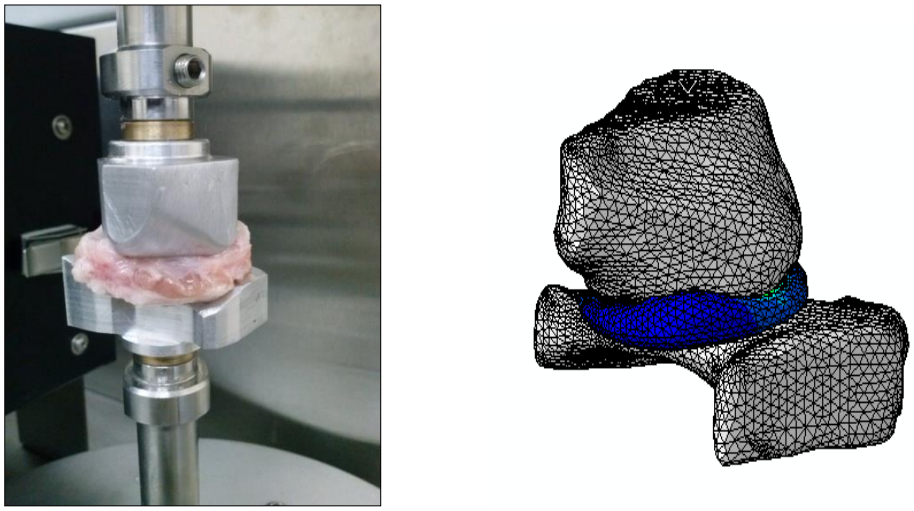

Figure 3. Whole disc in the testing tool and finite element model of the test.

To obtain the κ factor for effective crossed-sectional area (A_{eff}) calculation, an iterative procedure was implemented until convergence between the experimental force (F_x) and the simulated force (F_s) was achieved. The previously estimated experimental contact area (A_c) was also used during inverse material characterization to estimate the linear elastic Poisson ratio of the disc. The steps followed in the iterative procedure are presented in Figure 4.

Iterative inverse material characterization yielded κ value of 4.97 ± 0.17, meaning that the effective area was approximately five times smaller than the measured experimental contact area.

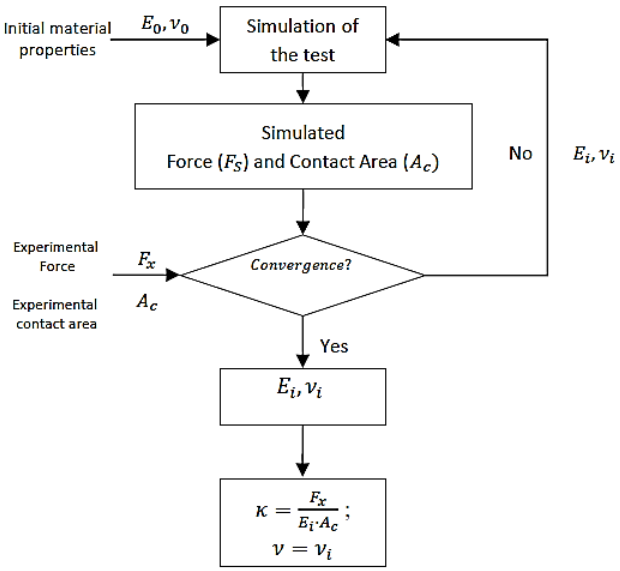

Figure 4. Schematic flow diagram of the inverse material characterization procedure, where E_0=0.032 MPa and ν_0=0.4.

2.4 **Dynamic compressive test**

The specimens were tested at room temperature under compression in a dynamic mechanical analysis Instrument (RSA3; TA Instruments) using the bone shaped fixture described in section 2.2. During the tests, the discs were lubricated. The compressive forces and distance between testing fixture surfaces were measured instantaneously using a load cell and linear variable transducer, respectively. Before initiating the testing protocol, the two surfaces of the testing fixture were allowed to contact each other to establish a zero value for thickness. Then, the fixture was opened and the disc was positioned between the two surfaces. A steady contact preload of 5 mN was then applied to the disc to ensure adequate whole specimen-fixture contact. With the preload of 5 mN applied, a thickness measurement was obtained at the thinnest part of the disc as a reference, enabling application of the desired strain during testing.

After the first steady contact period, a 3-min preconditioning test was performed with 1% sinusoidal strain before dynamic testing. After establishing a new steady contact, compression was applied to the specimen using a sinusoidal strain of $\varepsilon = \varepsilon_0 \sin(\omega t)$, where ω is the angular

velocity at each frequency. The administrative strain was ε_0 = 1% and the stress occurring was also described by a sinusoidal wave: $\sigma = \sigma_0 \sin(\omega t + \delta)$, where δ is the phase between strain application and stress measurement. The oscillation frequency ranged from 0.01 to 10 Hz (0.01, 0.05, 0.1, 0.5, 1, 2, 5, and 10 Hz) and the dynamic moduli were estimated and registered.

The above-described relationship between stress and strain can be employed to express the viscoelastic behavior of the disc using several parameters. As a result of the dynamic behavior of stress and strain, the compressive storage modulus (E'), the compressive loss modulus (E"), and the loss tangent (tan δ) were determined as dynamic viscoelastic parameters. E' represents the elastic component of the material behavior and E" represents the viscous component. The ratio of E'' to E' is given as tan δ.

2.5 Compressive stress relaxation test

Compression was applied to the specimens up to the specific strain using the same equipment as in the dynamic tests (RSA3; TA Instruments). The experimental configuration and procedure were the same as for dynamic testing. As there was no damage in the samples after the dynamic test, the same discs were used in the relaxation test. After changing the order of the tests, no influence in the results was observed.

First, the disc was placed atop the fossa surface and indented using the condyle surface of the fixture. The disc was compressed by displacement of the fossa component. The compressive force and distance between the fossa and condyle components were measured simultaneously.

After a series of dynamic tests, the compressive relaxation test was carried out at a strain level of 1% to obtain the corresponding relaxation modulus [$E_R(t)$]. The specific level of compressive strain was produced under an instantaneous strain step, and was kept constant during the 5 min period for each stress relaxation test. Loads were measured simultaneously under the specified constant strain.

3. Results

The results of dynamic compression testing showed that the storage (E') and loss (E'') moduli increased proportionally with frequency (Figures 5 and 6). While for the loss modulus, the total variation respect to maximum value is about 63%, the storage modulus values present a slight lower total change about 56%.

On the other hand, since the loss modulus remains almost constant and the storage modulus increases from 0.01 to 1 Hz, tan δ values decreases with frequency in that range.

From 1 to 10 Hz, tan δ clearly increased with frequency about 25% respect to the maximum value. As the Figure 7 shows, tan δ values ranged approximately from 0.2 to 0.3, indicating that the viscosity capacity of the disc cannot be neglected.

Static compression tests provided the Young's modulus of the whole disc over time (E_R; Figure 8). Relaxation of the modulus (E_R) of the whole disc over time is a clearly identifiable and common property of viscoelastic material behavior. As expected in viscoelastic behavior, a large amount of relaxation is observed for short periods (<0.1 s), and the relaxation rate slows with time until complete relaxation of the material occurs for long periods.

The results of static and dynamic testing allowed us to infer the viscoelastic behavior of the disc. Therefore, the results are consistent. Moreover, although the disc's loss modulus cannot be neglected, rough comparison of the dynamic storage and relaxation moduli can be performed; for example, for the intervals of 0.1-10 s and 10-0.1 Hz, approximate values of both moduli were 40-100 kPa, indicating that the results are in good agreement.

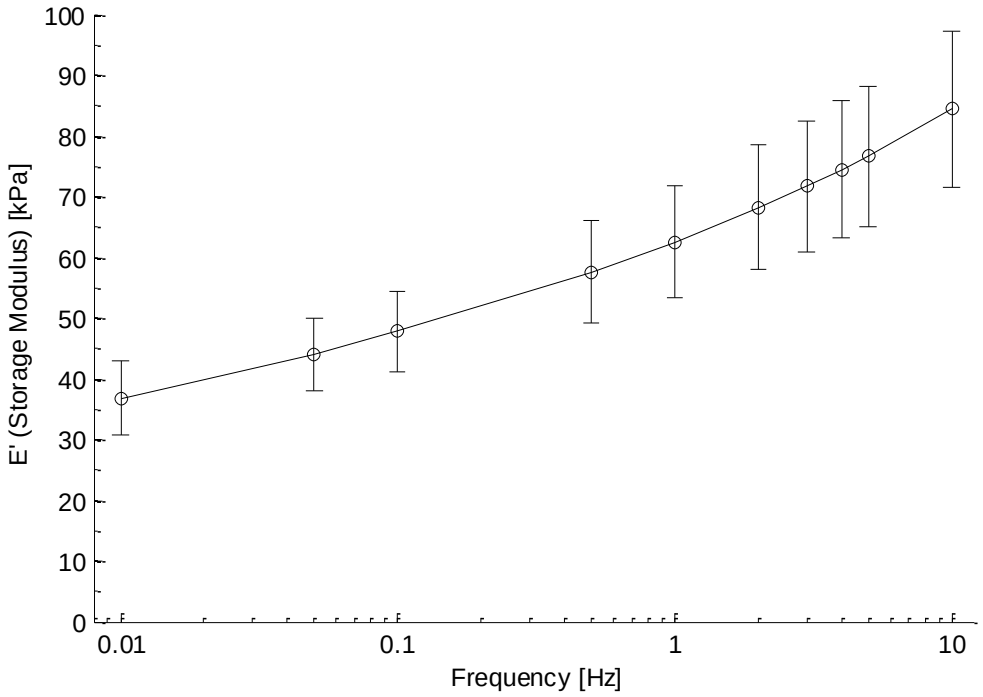

Figure 5. Storage moduli for the tested discs (n = 10).

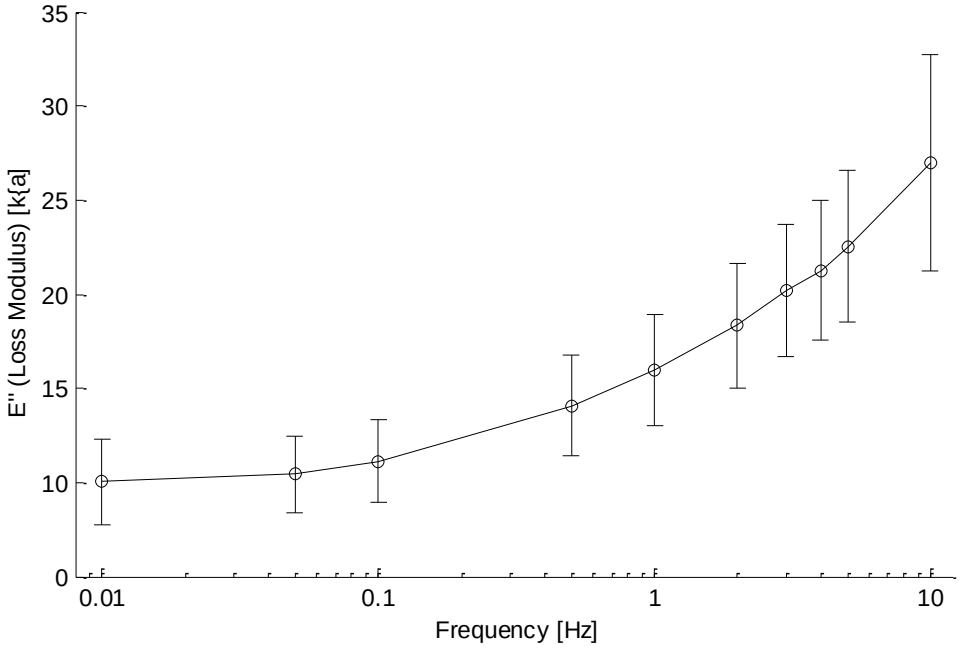

Figure 6. Loss moduli for the tested discs (n = 10).

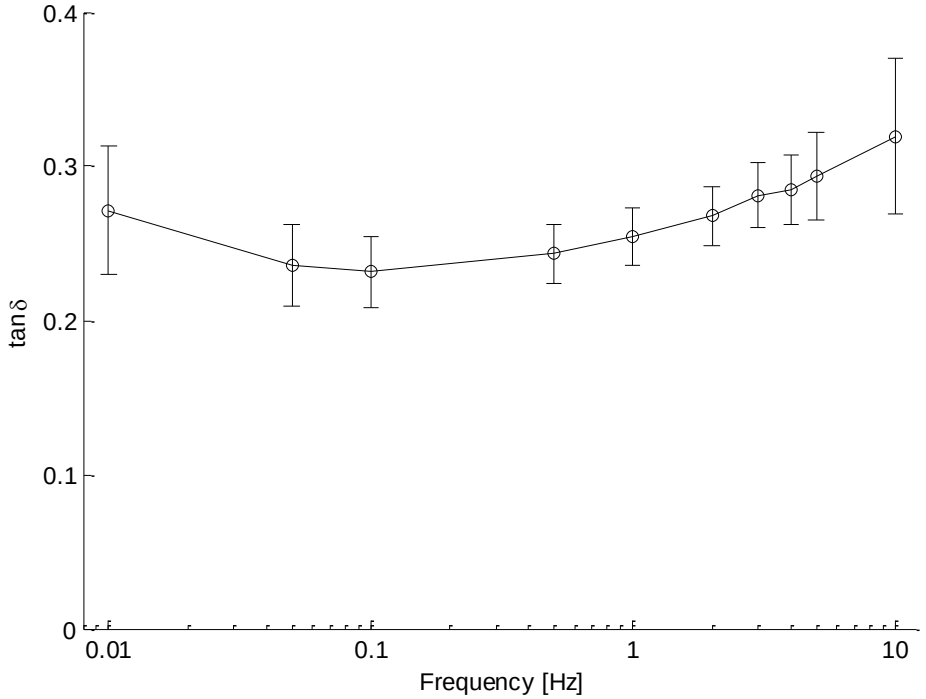

Figure 7. Tan δ values for the tested discs (n = 10).

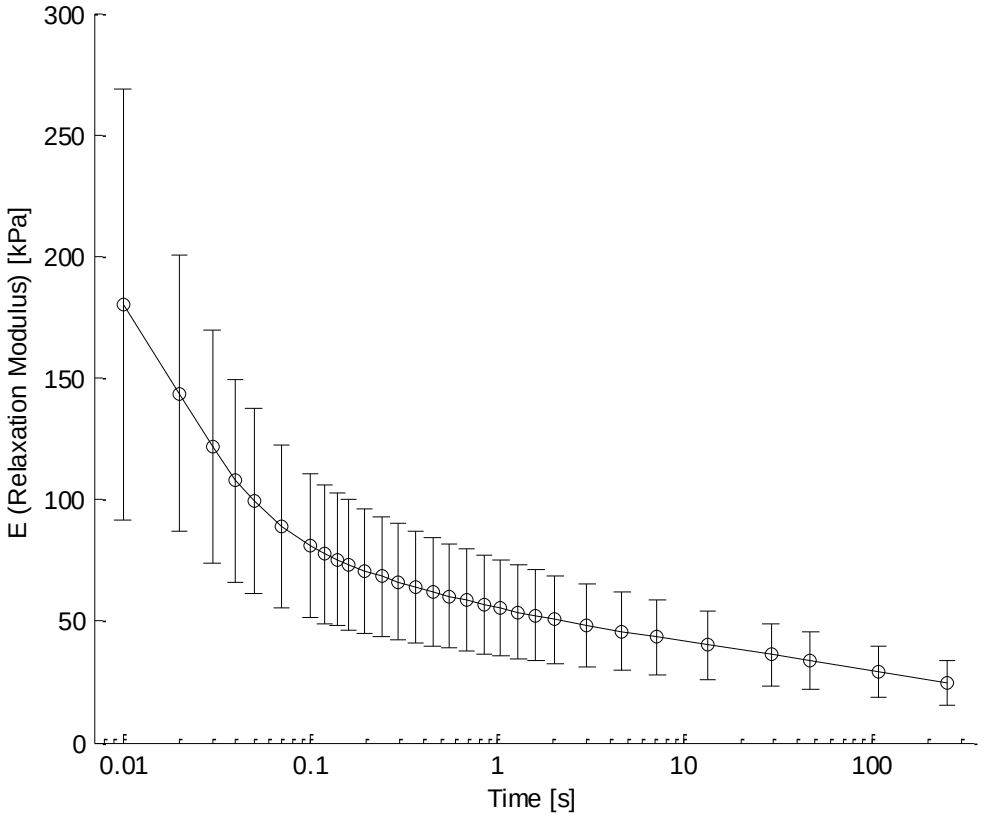

Figure 8. Relaxation moduli for the tested discs (*n* = 10).

7. Discussion

Numerous studies of TMJ articular cartilage behavior have involved static and dynamic measurement under compression to evaluate the mechanical properties of the disc at different strain rates and levels, frequencies, and/or time intervals (Beek et al., 2001; Hagandora et al., 2011; Tanaka et al. 2003, 2006, 2014; Allen and Athanasiou, 2006; Lamela et al. 2011, 2013; Pelayo et al., 2012) However, the complex geometry of the TMJ disc and the inhomogeneous distribution of material lead to the use of cut (i.e., cylindrical) specimens under confined or unconfined conditions. Although cut specimens simplify testing and facilitate comprehension of the regional mechanical properties of the disc, they do not aid the understanding of complete disc behavior. Thus, no information about the static and dynamic behaviors of the whole disc under compression is available. To our knowledge, the present study is the first to examine the static and dynamic viscoelastic properties of the whole TMJ disc under compression. In addition, the new testing tool developed in this study can be applied to enhance understanding of other biological tissues behavior.

In this study, we evaluated the static and dynamic viscoelastic behavior of the whole TMJ disc at a 1% compressive strain level. A comprehensive range of frequencies from 0.01 to 10 Hz was used for dynamic testing, and the relaxation time was set to 100 s for analysis of the disc's relaxation behavior over time. Our measurements were not performed at body temperature but at room temperature (about 30 ^{o}C). The dynamic properties of the TMJ disc are borne by the collagen and proteoglycan components, which are temperature sensitive. A higher temperature (the body temperature of a pig is about 39 ^{o}C) may slightly reduce stiffness and strength of the disc (Detamore and Athanasiou, 2003; Tanaka and van Eijden, 2003).

The indentation frequencies and strain applied in the present study cover various functional conditions in the human TMJ (Druzinsky, 1993; Kuboki et al., 1999; Gallo et al., 2000; Langenbach and van Eijden, 2001). Static and dynamic testing results indicated that the whole disc presented a viscoelastic behavior under compression. E' and E'' increased with frequency, and E_R decreased with time (see Figures 6 – 8). These results are consistent with viscoelastic behavior. During function, the mutual positions of the joint surfaces change, and the TMJ disc is subject to a multitude of different loading regimens during mandibular movements. Basically, three types of loading, namely, compression, tension, and shear, can be thereby distinguished. During static clenching grinding and so on, the TMJ disc is subject to compression and shear with much contact areas between the TMJ disc and articular cartilages; during dynamic tasks, such as chewing or talking, the amount of compressive and tensile strains will be much smaller with a small contact area. Since mandibular condyle always moves dynamically, the dynamic properties during chewing and talking may be representative for the disc. To evaluate the dynamic properties of the whole disc, further studies in the other configurations should be conducted in future.

Moreover, rough comparison (neglecting E") between E_R and E' revealed than these values were in the same range (40-100 kPa) in the same time and frequency intervals (0.1-10 s and 10-0.1 Hz, respectively), implying good correlation of findings from the different tests.

Although natural scatter is always present in data from biological tissues, the testing of whole discs provided testing cut specimens (Pelayo et al. 2012). Thus, the testing technique developed in this study can reduce uncertainty in the results of biological tissue testing.

The storage (E') and loss (E'') moduli obtained in the present study are of the same order of magnitude as those measured previously in cut disc specimens (Pelayo, et al., 2012). These values were slightly (about 10-15 kPa) higher for the whole disc compared with the averages of all regional moduli (Pelayo et al. 2012). This difference may be due to the simultaneous

compression and load supporting of all contact regions in the whole disc. No fiber or material was cut - no artificial damage was induced by cutting specimens allowing the natural flow of liquid inside the disc. This approach enabled us to observe more realistic and homogenous disc behavior, with compact mechanical properties, resulting in greater a stiffness under compression.

In conclusion, the dynamic and static properties of the porcine whole TMJ disc were determined under compression in this study. The dynamic compressive moduli increased with frequency, and these values were slightly higher than those obtained from cut disc specimens. Tan δ values ranged from 0.2 to 0.3, indicating that the behavior of the whole disc is primarily elastic, with small, but not negligible, viscosity. A novel testing device representing the mandibular condyle and glenoid fossa was designed and used in the experiments to provide more realistic functional conditions. Characterization of the material properties of the entire disc will aid with the interpretation of stress distribution on the TMJ as stress transmission between the fossa and condyle.

Acknowledgements

This research was supported in part by Grants-in-Aid 26293436 (E.T.) for Science Research from the Ministry of Education, Culture, Sports, Science and Technology, Japan. The funder had no role in study design, data collection and analysis, decision to publish, or preparation of the manuscript. The authors would also like to acknowledge the support of Dr. Santiago Llorente´s Clinic (Oviedo. Spain) during the tomographic analysis of this work and the funds granted by CajAstur Fellowship-University of Oviedo 2011 program.

References

Allen, K.D., Athanasiou, K.A., 2006. Viscoelastic characterization of the porcine temporomandibular joint disc under unconfined compression. J Biomech 39, 312-322.

Beek, M., Aarnts, M.P., Koolstra, J.H., Feilzer, A.J., van Eijden, T.M., 2001. Dynamic properties of the human temporomandibular joint disc. J Dent Res 80, 876-880.

Chen, J., Akyuz, U., Xu, L., Pidaparti, R.M.V., 1998. Stress analysis of the human temporomandibular joint. Med Eng Phys 20, 565-572.

Choi, A. P. C., Zheng, Y.P., 2005. Estimation of Young's modulus and Poisson's ratio of soft tissue from indentation using two different-sized indentors: finite element analysis of the finite deformation effect. Med Biol Eng Comput 43, 258-264.

Commisso, M.S., Martinez-Reina, J., Mayo, J., Dominguez, J., Tanaka, E., 2014. Effect of non-uniform thickness of samples in stress relaxation tests under unconfined compression of samples of articular discs. J Biomech 47, 1526-1530.

Detamore, M.S., Athanasiou, K.A., 2003. Structure and function of the temporomandibular joint disc: implications for tissue engineering. J Oral Maxillofac Surg 61, 494-506.

Druzinsky, R.E., 1993. The time allometry of mammalian chewing movements: chewing frequency scales with body mass in mammals. J Theor Biol 160, 427-440.

Gallo, L.M., Nickel, J.C., Iwasaki, L.R., Palla, S., 2000. Stress-field translation in the healthy human temporomandibular joint. J Dent Res 79, 1740-1746.

Hagandora, C.K., Chase, T.W., Almarza, A.J., 2011. A comparison of the mechanical properties of the goat temporomandibular joint disc to the mandibular condylar cartilage in unconfined compression. J Dent Biomech 212385.

Hattori-Hara, E., Mitsui, S.N., Mori, H., Arafurue, K., Kawaoka, T., Ueda, K., Yasue, A., Kuroda, S., Koolstra, J.H., Tanaka, E., 2014. Influence of unilateral disc displacement on stress in the contralateral joint with normally-positioned disc in human temporomandibular joint. J Cranio-Maxillo-Fac Surg 42, 2018-2024.

Ingawalé, S., Goswami, T, 2009. Temporomandibular Joint: Disorders, Treatments, and Biomechanics. Ann Biomed Eng 37, 976-996.

Kuboki, T., Takenami, Y., Orsini, M.G., Maekawa, K., Yamashita, A., Azuma, Y., Clark, G.T., 1999. Effect of occlusal appliances and clenching on the internally deranged TMJ space. J Orofac Pain 13, 38-48.

Kuo, J., Zhang, L., Bacro, T., Yao, H., 2010. The region-dependent biphasic viscoelastic properties of human temporomandibular joint discs under confined compression. J Biomech 43, 1316-1321.

Lamela, M.J., Prado, Y., Fernández, P., Fernández-Canteli, A., Tanaka, E., 2011. Non-linear Viscoelastic model for behaviour characterization of temporomandibular joint discs. Exp Mech 51, 1435-1440.

Lamela, M.J., Pelayo, F., Ramos, A., Fernandez-Canteli, A., Tanaka, E., 2013. Dynamic compressive properties of articular cartilages in the porcine temporomandibular joint. J Mech Behav Biomed Mater 23, 62-70.

Langenbach, G., van Eijden, T.M., 2001. Mammalian feeding motor patterns. Am Zool 41, 1338–1351.

Liu, Y., Kerdok, E.A., Howe, R.D., 2004. A Nonlinear Finite Element Model of Soft Tissue Indentation. Lec Note Comput Sci 3078, 67-76.

Pelayo, F., Lamela, M.J., Ramos, A., Fernández-Canteli, A., Tanaka, E., 2012. The región-dependent dynamic properties of porcine temporomandibular joint disc under unconfined compression. J Biomech 46, 845-848.

Pérez del Palomar, A., Doblaré, M., 2006. Finite element analysis of the temporomandibular joint during lateral excursions of the mandible. J Biomech 39, 2153-2163.

Tanaka, E., van Eijden, T., 2003. Biomechanical behavior of the temporomandibular joint disc. Crit Rev Oral Biol Med 14, 138-150.

Tanaka, E., Kikuzaki, M., Hanaoka, K., Tanaka, M., Sasaki, A., Kawai, N., et al., 2003. Dynamic compressive property of porcine temporomandibular joint disc. Eur J Oral Sci 111, 434-439.

Tanaka, E., del Pozo, R., Tanaka, M., Asai, D., Hirose, M., Iwabe, T., Tanne, K., 2004. Three-dimensional finite element analysis of human temporomandibular joint with and without disc displacement during jaw opening. Med Eng Phys 26, 508-511.

Tanaka, E., Hirose, M., Yamano, E., Dalla-Bona, D.A., Fujita, R., Tanaka, M., et al., 2006. Age-associated changes in viscoelastic properties of the bovine temporomandibular joint disc under compressive stress-relaxation. Eur J Oral Sci 114, 70-73.

Tanaka, E., Detamore, M.S., Tanimoto, K., Kawai, N., 2008. Lubrication of the temporomandibular joint. Ann Biomed Eng 36, 14-29.

Tanaka, E., Pelayo, F., Kim, N., Lamela, M.J., Kawai, N., Fernandez-Canteli, A., 2014. Stress relaxation behaviors of articular cartilages in porcine temporomandibular joint. J Biomech 47, 1582-1587.

Zheng, Y., Mak, A.F.T., Lue, B., 1999. Objective assessment of limb tissue elasticity: Development of a manual indentation procedure. J Rehabil Res Dev 26, 2.

Figure Captions:

Figure 1. Design of the fixture tool used whole disc tests and steps in the manufacturing process. STL, stereolithographic.

Figure 2. Procedure for obtaining the contact area (A_c) between the condyle (indenter) and the discs. From the left to the right: Condyle tool with the print of the contact area; 3D model of the condyle with the 3D polyline used; Overlap of the Real print and the 3D print.

Figure 3. Whole disc in the testing tool and finite element model of the test.

Figure 4. Schematic flow diagram of the inverse material characterization procedure, where E_0=0.032 MPa and v_0=0.4.

Figure 5. Storage moduli for the tested discs (n = 10).

Figure 6. Loss moduli for the tested discs (*n* = 10).

Figure 7. Tan δ values for the tested discs (*n* = 10).

Figure 8. Relaxation moduli for the tested discs (*n* = 10).